

Electromagnetic Surface Waves in Microwave Absorbing Layers

Electromagnetic Surface Waves in Microwave Absorbing Layers

By

Pyotr Ya. Ufimtsev, Rung T. Ling
and Gokhan Apaydin

Cambridge
Scholars
Publishing



Electromagnetic Surface Waves in Microwave Absorbing Layers

By Pyotr Ya. Ufimtsev, Rung T. Ling and Gokhan Apaydin

This book first published 2024

Cambridge Scholars Publishing

Lady Stephenson Library, Newcastle upon Tyne, NE6 2PA, UK

British Library Cataloguing in Publication Data

A catalogue record for this book is available from the British Library

Copyright © 2024 by Pyotr Ya. Ufimtsev, Rung T. Ling
and Gokhan Apaydin

All rights for this book reserved. No part of this book may be reproduced, stored in a retrieval system, or transmitted, in any form or by any means, electronic, mechanical, photocopying, recording or otherwise, without the prior permission of the copyright owner.

ISBN (10): 1-0364-0426-9

ISBN (13): 978-1-0364-0426-0

TABLE OF CONTENTS

List of Illustrations	vii
Acknowledgment.....	xi
Preface	xiii
Abstract	xv
Introduction	1
Chapter One.....	5
General Properties of Surface Waves	
1.1 Basic field equations	
1.2 Dispersion equations as zeroes or poles of reflection coefficients	
1.3 Phase and amplitude fronts of surface waves	
1.4 New definition for the phase velocity of surface waves	
1.5 New definition for the energy velocity of surface waves	
1.6 Spatial distribution of the power fluxes in surface waves	
Chapter Two	33
New Physical Phenomena Related to Surface Waves	
2.1 Attenuation and losses of surface waves	
2.2 Upper frequency cutoff	
2.3 Shifting of the upper frequency cutoff	
2.4 Merging of high order modes	
Chapter Three	55
Transformation and Excitation of Surface Waves in Absorbing Layers	
3.1 Rotation of the Poynting vector in the complex plane of the transverse wave number	

3.2 Diagrams of guided waves	
3.3 Absence of standing damped guided waves in absorbing layers	
3.4 Continuous transformations of surface waves in absorbing layers	
3.5 Excitation of surface waves in thin absorbing layers	
3.6 Summary and Conclusion	
Appendix	87
References	89
Biography	93

LIST OF ILLUSTRATIONS

- Fig. 1-1 Absorbing layer ($0 \leq y \leq a$) backed up by a perfectly conducting plane ($y = 0$).
- Fig. 1-2 Constitutive properties of sample material (constant relative permittivity: $\epsilon' = 20.45$, $\epsilon'' = 0.73$).
- Fig. 1-3 Reflection of the plane wave by the layer.
- Fig. 1-4 Amplitude and phase fronts of the surface wave above the layer.
- Fig. 1-5 Phase front angles of TM-waves outside the layers.
- Fig. 1-6 Amplitude front angles of TM-waves outside the layers.
- Fig. 1-7 Imaginary part of the Brewster angle for TM-waves.
- Fig. 1-8 Phase front angles of TE-waves outside the layers.
- Fig. 1-9 Imaginary part of the Brewster angle for TE-waves.
- Fig. 1-10 Structure of surface waves inside the layer.
- Fig. 1-11 Phase front angles of TM-waves inside the layers.
- Fig. 1-12 Amplitude front angles of the TM-wave inside the layers.
- Fig. 1-13 Angles between phase front and amplitude front of the TM-wave inside the layers.
- Fig. 1-14 Angles between phase front and amplitude front of the TE-wave inside the layers.
- Fig. 1-15 Phase velocity of TM surface waves outside the layers.
- Fig. 1-16 Phase velocity of TE surface waves outside the layers.
- Fig. 1-17 Conventional phase velocity of TM-waves.
- Fig. 1-18 Conventional phase velocity of TE-waves.
- Fig. 1-19 Conventional group velocity of TM-waves.
- Fig. 1-20 P_2 / P_1 ratio for TM-waves.
- Fig. 1-21 P_2 / P_1 ratio for TE-waves.
- Fig. 1-22 Definition of the angle $\phi(y)$.
- Fig. 1-23 Streamlines of the power flux inside the layer. TM surface waves. Layer thickness 0.05".
- Fig. 1-24 Streamlines of the power flux inside the layer. TE surface waves. Layer thickness 0.07".

- Fig. 2-1 Attenuation constant α_e (electric loss) for TM surface waves in absorbing layers.
- Fig. 2-2 Attenuation constant α_m (magnetic loss) for TM surface waves in absorbing layers.
- Fig. 2-3 Total attenuation constant of TM-waves in absorbing layers.
- Fig. 2-4 Attenuation constant of TM surface waves as a function of the ratio a / λ_d .
- Fig. 2-5 Attenuation constant α_e (electric loss) for TM surface waves in absorbing layers.
- Fig. 2-6 Attenuation constant α_m (magnetic loss) for TE surface waves in absorbing layers.
- Fig. 2-7 Total attenuation constant of TE-waves in absorbing layers.
- Fig. 2-8 Attenuation constant of TE-waves as a function of the ratio a / λ_d .
- Fig. 2-9 Real part of the transverse wavenumber for TM-waves.
- Fig. 2-10 Imaginary part of the transverse wavenumber for TM-waves.
- Fig. 2-11 Real part of the propagation constant for TM-waves.
- Fig. 2-12 Imaginary part of the propagation constant for TM-waves.
- Fig. 2-13 Geometrical interpretation of dispersion equations for surface waves in the layers without loss: a) TM-waves, b) TE-waves.
- Fig. 2-14 Real part of the transverse wave number for TE-waves.
- Fig. 2-15 Imaginary part of the transverse wave number for TE-waves.
- Fig. 2-16 Real part of the propagation constant for TE-waves.
- Fig. 2-17 Imaginary part of the propagation constant for TE-waves.
- Fig. 2-18 Demonstration of the upper cutoff phenomenon for TE-waves in the absorbing layer with a thickness $a = 0.30''$. Original ε and μ shown in Fig. 1-2.
- Fig. 2-19 Attenuation constants of TM surface waves in layers with constitutive parameters 120% of original ε and μ shown in Fig. 1-2.
- Fig. 2-20 Attenuation constants of TM surface waves in layers with original ε and μ shown in Fig. 1-2.
- Fig. 2-21 Attenuation constants of TM surface waves in layers with constitutive parameters 80% of original ε and μ shown in Fig. 1-2.

Fig. 2-22 Attenuation constants of TE surface waves in layers with constitutive parameters 120% of original ϵ and μ shown in Fig. 1-2.

Fig. 2-23 Attenuation constants of TE surface waves in layers with original ϵ and μ shown in Fig. 1-2.

Fig. 2-24 Dispersion curves of TE surface waves in the absorbing layer with constitutive parameters 1.3ϵ and 1.3μ where ϵ and μ are shown in Fig. 1-2. Layer thickness 0.30". The transverse wave numbers of these waves are located in the second quadrant on the first Riemann sheet in the complex k_t -plane.

Fig. 2-25 Dispersion curves of TE surface waves in the absorbing layer with constitutive parameters 1.35ϵ and 1.35μ where ϵ and μ are shown in Fig. 1-2. Layer thickness 0.30".

Fig. 2-26 Dispersion curves of TE surface waves in the absorbing layer with constitutive parameters 1.5ϵ and 1.5μ where ϵ and μ are shown in Fig. 1-2. Layer thickness 0.30".

Fig. 2-27 Dispersion curves of TE surface waves in the absorbing layer with constitutive parameters 1.8ϵ and 1.8μ where ϵ and μ are shown in Fig. 1-2. Layer thickness 0.30".

Fig. 3-1 The first Riemann sheet ($\text{Im}(\beta) \geq 0$).

Fig. 3-2 The second Riemann sheet ($\text{Im}(\beta) \leq 0$).

Fig. 3-3 Rotation of the Poynting vector on the contour which intersects branch cuts two times.

Fig. 3-4 Rotation of the Poynting vector on the contour which intersects branch cuts four times.

Fig. 3-5 The diagram of guided waves in the first Riemann sheet ($\text{Im}(\beta) \geq 0$).

Fig. 3-6 The diagram of guided waves in the second Riemann sheet ($\text{Im}(\beta) \leq 0$).

Fig. 3-7 Continuous transformation of surface waves.

Fig. 3-8 Trajectories of the transverse wave number of fundamental TM guided waves in absorbing layers. The oscillation frequency ($f = ck_0 / 2\pi$) increases in the counter-clockwise direction along each trajectory.

Fig. 3-9 Trajectories of the transverse wave number of fundamental TE guided waves in absorbing layers. The oscillation frequency ($f = ck_0 / 2\pi$) increases from the bottom to the top along each trajectory.

Fig. 3-10 Trajectories of the transverse wave number of three TE guided waves. Layer thickness 0.075". The directions at which the oscillation frequency ($f = ck_0 / 2\pi$) increases along each trajectory are shown by arrows.

Fig. 3-11 Dispersion curves of TE-wave modes in the absorbing layer with constitutive parameters shown in Fig.1-2. Layer thickness 0.075". The lower curve belongs to the leaky wave.

Fig. 3-12 Surface impedance for TM-waves. Layer thickness 0.05", frequency 2 GHz.

Fig. 3-13 Surface impedance for TE-waves. Layer thickness 0.3", frequency 11.44 GHz.

Fig. 3-14 Surface impedance calculated by eqs. (3.14) - (3.16). Layer thickness 0.05", incidence angle $\theta = 90^\circ$. Denotations: $\bullet \text{Re}(Z_{refl}^{TE})$, $\blacktriangle \text{Im}(Z_{refl}^{TE})$, $\blacksquare \text{Re}(Z_{refl}^{TM})$, $\blacklozenge \text{Im}(Z_{refl}^{TM})$, $\blacktriangledown \text{Re}(Z_{sw}^{TM})$, $\circ \text{Im}(Z_{sw}^{TM})$.

Fig. 3-15 Excitation of surface waves by the aperture limited plane wave.

Fig. 3-16 Branch cuts in the complex plane (ζ) and the integration contour in eq. (3.21).

Fig. 3-17 Launching efficiency of TM surface waves at 2 GHz. Launching aperture height $h = 1$ m.

Fig. 3-18 $(P_1 + P_2) / P^{refl}$ ratio for TM-waves at 2 GHz. Launching aperture height $h = 1$ m.

Fig. 3-19 Launching efficiency of TE surface waves at 11.44 GHz. Layer thickness 0.3". Launching aperture height $h = 1$ m.

Fig. A-1 Debye model fit for permeability.

ACKNOWLEDGMENT

The authors are thankful to Dr. A. D. Varvatsis who provided the Debye approximation for permeability of the absorbing material analyzed in this book. This research project was supported in parts by the University of California at Los Angeles (USA), the Technical University at Hamburg (Germany), and the Northrop Grumman Corporation (USA).

PREFACE

The objective of this book is to analyze surface waves in absorbing layers used for the purpose of reducing the radar cross sections (RCS). These waves are originally generated by radars at geometrical or material discontinuities on the target surface. They propagate into absorbing coatings where they are transformed into heat energy. In accordance with the reciprocity principle, they can also turn into radiation when encountering such inhomogeneities in the target surface. Thus, surface waves represent a constitutive part of the complex scattering and absorption process. However, their physical properties have not been studied in detail despite the fact that absorbing coatings have widely been used since the Second World War. They have now been investigated in detail by the authors. We have discovered some new physical phenomena, such as upper frequency cutoff limits, the shifting of these cutoff limits to higher frequencies in material with smaller losses, and the merging of high order modes. These and other new results are presented and analyzed in this book. They are useful for electrical engineers and scientists interested in surface waves phenomena and in microwave absorbing material, as well as in lossy microwave circuits.

ABSTRACT

Surface waves are well investigated in problems related to propagation of elastic, acoustic, radio, and optics waves. But this is not the case with surface waves in microwave absorbing materials. In spite of the fact that radar absorbing coatings have been widely used since the Second World War, the properties of surface waves, which can exist in such materials, have not been studied in detail. Currently available books provide a general description of surface and other types of guided waves and focus mostly on the problems which do not relate directly to surface waves in microwave coatings. Analysis of radar absorbing materials (RAM) in technical books is usually based on the evaluation of the reflection coefficient only. However, surface waves play an important role in the absorption of radar waves. These waves also can provide an appreciable contribution to a fine structure of the scattered field when they transform into radiated waves at edges and material discontinuities. It was the authors' intention to fill in the gap in the existing theory of surface waves by investigating their properties in microwave absorbing materials. In this book, the authors present new results for surface waves in actual absorbing layers.

It has been shown that the traditional notions of the phase velocity and group velocity widely used in the theory of transmission lines are inappropriate for surface waves in absorbing layers. New, more general and appropriate definitions based on a physical view point for the phase velocity and energy velocity have been introduced. Physical phenomena hitherto unknown have been discovered and described. These include the upper frequency cutoff of surface waves, shifting of this cutoff to higher frequencies in materials with lower losses, and merging of high order surface waves / modes. These and other new results are presented and analyzed in this book. They can be of interest to the designers of radar absorbing coatings, microwave transmission lines and microwave devices.

INTRODUCTION

Surface waves represent a special class of guided waves. A distinctive feature of these waves is an exponential decrease of their amplitude in the direction normal to and away from the guiding structure. These waves were first discovered theoretically by Sommerfeld [1, 2] and Zenneck [3]. Sommerfeld investigated surface waves supported by thin imperfect cylindrical conductors. Zenneck studied surface waves near a flat interface between two homogeneous media. Goubau demonstrated experimentally surface waves propagating along metallic wires [4]. Since then, numerous articles were published about surface waves and now they have become a classic subject in the theory of guided waves [5-10, 15-18]. However, in this theory, transmission lines are usually considered without losses. Small losses are treated sometimes by the perturbation technique [18, 20].

As far as we know, properties of surface waves in actual absorbing structures with high losses were not well known. They were investigated by these authors in [21-25]. The results of these investigations, their analysis in detail and some other new results are presented in this book.

The first chapter contains the description of general properties of surface waves in absorbing layers. They include the physical structure of surface waves, the interpretation of them as inhomogeneous plane waves incident on the layer under the complex Brewster angles, and interpretations of dispersion equations as zeroes of the numerator or denominator of the reflection coefficient for the incident plane wave. It is also shown that the conventional notions of the phase and group velocities traditionally used in the theory of guided waves are not applicable in the case of actual absorbing material. Instead, we have introduced new physically reasonable and more general definitions for the phase velocity and the energy velocity.

Chapter 2 contains analysis of numerical results for attenuation and propagation constants of surface waves. It describes new physical phenomena discovered in [21-25] which do not exist in layers without

losses. These are the upper frequency cutoff, the shifting of this cutoff to higher frequencies in layers with lower losses, and the merging of high order modes.

Absorbing layers can support different types of guided waves. Special wave diagrams convenient for classification and analysis of guided waves are suggested in Chapter 3. Transformation of surface waves into other guided waves is investigated. In particular, it is shown that continuous transformation of surface waves into growing and leaky waves is forbidden.

In a single-mode frequency band, thin absorbing layers with appropriate parameters can be considered approximately as a plane with the standard impedance boundary condition. This approach is used in Chapter 3 to analyze the excitation of absorbing layers by an aperture-limited plane wave. An exact analytical solution of this problem is provided and analyzed. Numerical data for the launching efficiency of surface waves are presented.

In this book, we investigate surface waves in a homogeneous absorbing layer placed on a perfectly conducting plane (Fig. 1-1). Though this two-dimensional model is simple, it allows one to study some general properties of surface waves. Some results of this study are also valid for any stratified coatings. It should be noted that all numerical results were performed for an actual commercially available material with constitutive parameters shown in Fig. 1-2.

Such materials are widely used as microwave absorbing coatings. The Debye model-fit (A.1) for these experimental data was developed by Dr. A.D. Varvatsis and is presented in the Appendix. It is consistent with the Kramers-Kronig relations [19] and confirms the validity of experimental data. This material is ceramic in nature and it is embedded with small spherical metallic particles. Such materials are widely used as microwave absorbing coatings. Electromagnetic design and application of radar absorbing materials are presented in the Handbooks [27, 39].

In Fig. 1-1, the thickness of the layer is denoted by the letter a . Its relative permittivity and permeability are ε and μ , respectively. A free space ($\varepsilon = \mu = 1$) is assumed to be above the layer. The wave number in

free space is denoted as $k_0 = \omega \sqrt{\varepsilon_0 \mu_0} = 2\pi / \lambda_0$, ω is the angular frequency of harmonic oscillations and λ_0 is the free space wavelength. The time dependence $\exp(-i\omega t)$ is assumed and suppressed below.

CHAPTER ONE

GENERAL PROPERTIES OF SURFACE WAVES

1.1 Basic field equations

The geometry of the problem is shown in Fig. 1-1. Here, ε and μ are the relative permittivity and permeability, respectively. It follows from Maxwell's equations that two types of surface waves can exist in absorbing layers: the transverse magnetic (TM) and transverse electric (TE) waves. In TM-waves, the magnetic vector \vec{H} contains only the x-component (H_x), while in TE-waves only the x-component (E_x) of the electric vector \vec{E} can exist.

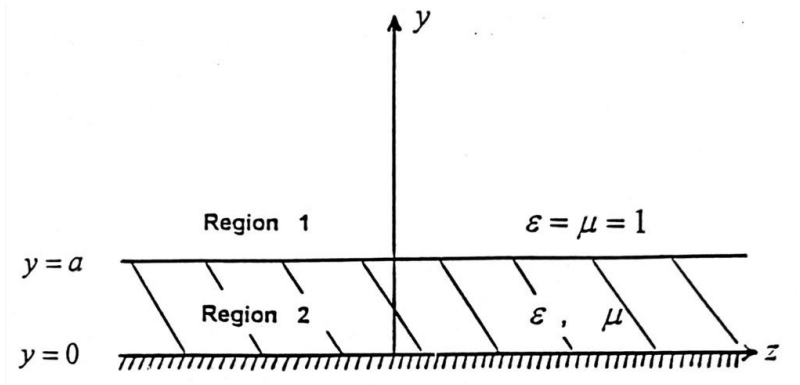


Fig. 1-1. Absorbing layer ($0 \leq y \leq a$) backed up by a perfectly conducting plane ($y = 0$).

The TM-waves are described by equations

$$H_x = e^{ik_1(y-a)} e^{i\beta z},$$

$$E_y = -\frac{\beta}{k_0} Z_0 H_x, \quad E_z = \frac{k_1}{k_0} Z_0 H_x, \quad (1.1)$$

$k_0 = \omega / c = \omega \sqrt{\varepsilon_0 \mu_0}$ in the free space (Region 1), $y \geq a$, and by equations

$$H_x = \frac{\cos(k_2 y)}{\cos(k_2 a)} e^{i\beta z},$$

$$E_y = -\frac{\beta}{k_0 \varepsilon} Z_0 H_x, \quad E_z = i \frac{k_2}{k_0 \varepsilon} Z_0 H_x \tan(k_2 y) \quad (1.2)$$

inside the layer (Region 2), $0 \leq y \leq a$. In these equations, $Z_0 = \sqrt{\mu_0 / \varepsilon_0}$ is the impedance of the free space. The complex quantities $k_2 = k_2' + ik_2''$ and $k_1 = k_1' + ik_1''$ are the transverse wave numbers of the wave field inside and outside the layer, respectively. The complex quantity $\beta = \beta' + i\beta''$ is the longitudinal wave number or the propagation constant. These wave numbers are connected by the relations

$$k_1^2 + \beta^2 = k_0^2, \quad k_2^2 + \beta^2 = k_0^2 \varepsilon \mu \quad (1.3)$$

through the Helmholtz wave equation. It follows that

$$k_2^2 - k_1^2 = k_0^2 (\varepsilon \mu - 1). \quad (1.4)$$

The H_x -components from eqs. (1.1) and (1.2) are continuous on top of the layer ($y = a$). The E_z -component satisfies the boundary condition on the perfectly conducting plane ($E_z = 0$ at $y = 0$) and its continuity on top of the layer, $y = a$ leads to a transcendental equation

$$k_1 \varepsilon = ik_2 \tan(k_2 a). \quad (1.5)$$

This transforms into the dispersion equation

$$D^{\text{TM}}(k_0, \beta) = \sqrt{k_0^2 \varepsilon \mu - \beta^2} \tan \left(a \sqrt{k_0^2 \varepsilon \mu - \beta^2} \right) + i \varepsilon \sqrt{k_0^2 - \beta^2} = 0 \quad (1.6)$$

with the substitutions of k_1 and k_2 from eq. (1.3).

The TE-waves are described by similar equations. Their field components above the layer ($y \geq a$) are

$$E_x = e^{ik_1(y-a)} e^{i\beta z},$$

$$H_y = \frac{\beta}{k_0} Y_0 E_x, \quad H_z = -\frac{k_1}{k_0} Y_0 E_x, \quad (1.7)$$

and inside the layer ($0 \leq y \leq a$), they are

$$E_x = \frac{\sin(k_2 y)}{\sin(k_2 a)} e^{i\beta z},$$

$$H_y = \frac{\beta}{k_0 \mu} Y_0 E_x, \quad H_z = i \frac{k_2}{k_0 \mu} Y_0 E_x \cot(k_2 y), \quad (1.8)$$

where $Y_0 = 1/Z_0$ is the admittance of free space.

The wave numbers k_1 , k_2 , β of TE-waves also obey eqs. (1.3) and (1.4). But instead of eq. (1.5) for TM-waves, they satisfy the dispersion equation

$$k_1 \mu = -ik_2 \cot(k_2 a) \quad (1.9)$$

which can be written as

$$D^{\text{TE}}(k_0, \beta) = \sqrt{k_0^2 \varepsilon \mu - \beta^2} \cot \left(a \sqrt{k_0^2 \varepsilon \mu - \beta^2} \right) + i \mu \sqrt{k_0^2 - \beta^2} = 0 \quad (1.10)$$

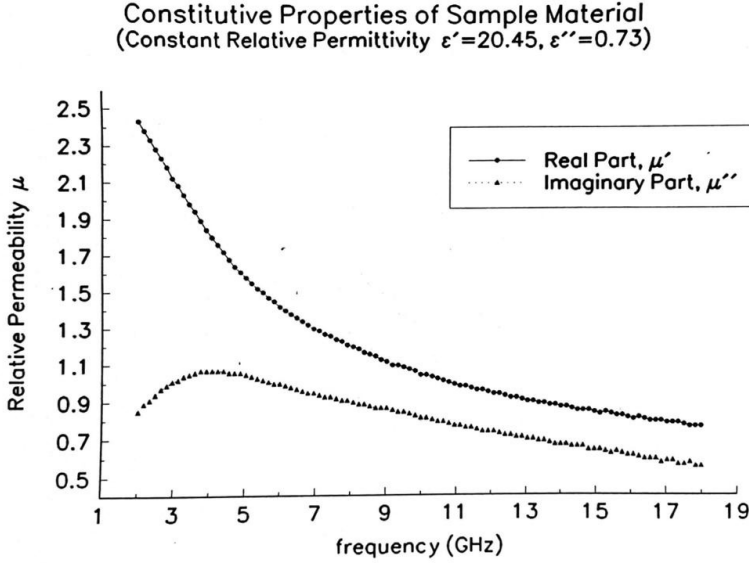


Fig. 1-2. Constitutive properties of sample material (constant relative permittivity: $\epsilon' = 20.45$, $\epsilon'' = 0.73$).

All numerical data presented in this book were obtained with the solutions of dispersion equations (1.6) and (1.10) using the Muller's method [28]. Constitutive parameters of a sample material are shown in Fig. 1-2.

For surface waves, the imaginary part of the transverse wave number k_1 is always positive thus ensuring an exponential decay of the field in the direction away from the layer. One should note that a tight connection exists between the dispersion equations (1.6), (1.10), and the reflection coefficients of plane waves incident on the layer. This connection is demonstrated in the next section.

1.2 Dispersion equations as zeroes or poles of reflection coefficients

First, consider the reflection of the TM plane wave

$$H_x^{\text{inc}} = e^{ik_0(z \cos \theta - y \sin \theta)} \quad (1.11)$$

from the homogeneous absorbing layer (Fig. 1-3). This is a classic problem considered in handbooks on Electromagnetics. We present here only the final expression for the reflected wave

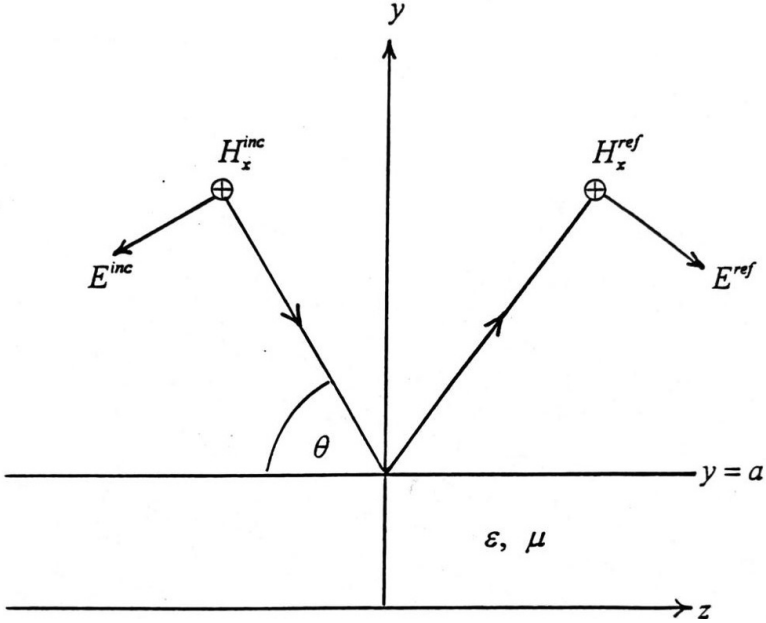


Fig. 1-3. Reflection of the plane wave by the layer.

$$H_x^{\text{ref}} = \rho_h(\theta) e^{ik_0(z \cos \theta + y \sin \theta)} e^{-i2k_0 a \sin \theta} \quad (1.12)$$

where the reflection coefficient $\rho_h(\theta)$ is given by

$$\rho_h(\theta) = \frac{\varepsilon \sin \theta + i\sqrt{\varepsilon\mu - \cos^2 \theta} \tan\left(k_0 a \sqrt{\varepsilon\mu - \cos^2 \theta}\right)}{\varepsilon \sin \theta - i\sqrt{\varepsilon\mu - \cos^2 \theta} \tan\left(k_0 a \sqrt{\varepsilon\mu - \cos^2 \theta}\right)}. \quad (1.13)$$

By setting $\cos \theta = \beta / k_0$ and $\sin \theta = -\sqrt{1 - (\beta / k_0)^2} = -k_1 / k_0$ with complex β determined by eq. (1.6), the incident plane wave given by eq. (1.11) transforms into eq. (1.1) for the surface wave. Here the angle θ can be recognized as the complement of the Brewster angle γ_B defined in the next section. The reflection coefficient changes into

$$\rho_h = \frac{i\varepsilon\sqrt{k_0^2 - \beta^2} + \sqrt{k_0^2\varepsilon\mu - \beta^2} \tan\left(a\sqrt{k_0^2\varepsilon\mu - \beta^2}\right)}{i\varepsilon\sqrt{k_0^2 - \beta^2} - \sqrt{k_0^2\varepsilon\mu - \beta^2} \tan\left(a\sqrt{k_0^2\varepsilon\mu - \beta^2}\right)}. \quad (1.14)$$

The numerator of this expression is exactly the left-hand side of the dispersion equation (1.6) and, therefore, it is equal to zero. This confirms the observations [5, 29], that the surface wave can be interpreted as an inhomogeneous plane wave incident on the guiding structure under the complex Brewster angle without reflection.

We also can transform the reflected wave (1.12) into the surface wave (1.1) by setting $\cos \theta = \beta / k_0$ and $\sin \theta = \sqrt{1 - (\beta / k_0)^2} = k_1 / k_0$.

In this case, the reflection coefficient changes to

$$\rho_h = \frac{i\varepsilon\sqrt{k_0^2 - \beta^2} - \sqrt{k_0^2\varepsilon\mu - \beta^2} \tan\left(a\sqrt{k_0^2\varepsilon\mu - \beta^2}\right)}{i\varepsilon\sqrt{k_0^2 - \beta^2} + \sqrt{k_0^2\varepsilon\mu - \beta^2} \tan\left(a\sqrt{k_0^2\varepsilon\mu - \beta^2}\right)}. \quad (1.15)$$

The denominator of this expression equals zero due to the dispersion equation (1.6). This pole of the reflection coefficient can be interpreted as the existence of the reflected wave (i.e. surface wave) in the absence of the incident wave.

Now let us consider the reflection of TE plane wave

$$E_x^{\text{inc}} = e^{ik_0(z \cos \theta - y \sin \theta)} \quad (1.16)$$

from the same layer. The reflected wave is determined as

$$E_x^{\text{ref}} = \rho_e(\theta) e^{ik_0(z \cos \theta + y \sin \theta)} e^{-i2k_0 a \sin \theta} \quad (1.17)$$

with the reflection coefficient

$$\rho_e(\theta) = \frac{\mu \sin \theta - i\sqrt{\varepsilon\mu - \cos^2 \theta} \cot(k_0 a \sqrt{\varepsilon\mu - \cos^2 \theta})}{\mu \sin \theta + i\sqrt{\varepsilon\mu - \cos^2 \theta} \cot(k_0 a \sqrt{\varepsilon\mu - \cos^2 \theta})}. \quad (1.18)$$

By setting $\cos \theta = \beta / k_0$ and $\sin \theta = -\sqrt{1 - (\beta / k_0)^2} = -k_1 / k_0$ with complex β determined by eq. (1.10), the incident plane wave (1.16) transforms into eq. (1.7) for the surface wave and the reflection coefficient changes into

$$\rho_e = \frac{i\mu\sqrt{k_0^2 - \beta^2} - \sqrt{k_0^2\varepsilon\mu - \beta^2} \cot(a\sqrt{k_0^2\varepsilon\mu - \beta^2})}{i\mu\sqrt{k_0^2 - \beta^2} + \sqrt{k_0^2\varepsilon\mu - \beta^2} \cot(a\sqrt{k_0^2\varepsilon\mu - \beta^2})}. \quad (1.19)$$

The numerator of this coefficient equals zero due to the dispersion equation (1.10). This means that the surface wave can be interpreted as the inhomogeneous plane wave incident on the layer under a complex Brewster angle. Again, the reflected wave (1.17) also can be considered as the surface wave by setting $\cos \theta = \beta / k_0$ and $\sin \theta = \sqrt{1 - (\beta / k_0)^2} = k_1 / k_0$.

In this case, the reflection coefficient changes into

$$\rho_e = \frac{i\mu\sqrt{k_0^2 - \beta^2} + \sqrt{k_0^2\varepsilon\mu - \beta^2} \cot(a\sqrt{k_0^2\varepsilon\mu - \beta^2})}{i\mu\sqrt{k_0^2 - \beta^2} - \sqrt{k_0^2\varepsilon\mu - \beta^2} \cot(a\sqrt{k_0^2\varepsilon\mu - \beta^2})}. \quad (1.20)$$

According to the dispersion equation (1.10), the denominator here equals zero. The infinite reflection coefficient means the existence of the reflected wave (i.e. the surface wave) in the absence of the incident wave. Thus, we see that dispersion equations can be interpreted as zeroes or poles of the reflection coefficients. This property of the reflection coefficients is used sometimes to derive dispersion equations.

1.3 Phase and amplitude fronts of surface waves

Equations (1.1) describe a spatial distribution of the surface wave outside the layer ($y > a$) with a factor

$$e^{i(\phi_p - \phi_a)} \text{ where } \phi_p = \beta'z + k_1'y, \phi_a = \beta''z + k_1''y. \quad (1.21)$$

For physically allowed solutions above the lower cutoff frequency, the dispersion equations provide the following values: $\beta' > 0$, $\beta'' \geq 0$, and $k_1' \leq 0$, $k_1'' > 0$. Therefore, the surface wave outside the absorbing layer is an inhomogeneous plane wave incident on the layer without reflection. Due to the losses inside the layer this wave undergoes the exponential attenuation in the z -direction and its amplitude decreases exponentially along the normal to the layer (in the y -direction).

Setting $\phi_p = \text{const}$ and $\phi_a = \text{const}$ determines the phase and amplitude fronts, respectively:

$$y_p = z_p \tan \gamma_p + \text{const}, \quad y_a = z_a \tan \gamma_a + \text{const}, \quad (1.22)$$

where

$$\tan \gamma_p = -\frac{\beta'}{k_1'}, \quad \tan \gamma_a = -\frac{\beta''}{k_1''}. \quad (1.23)$$

According to eq. (1.3), the quantity $k_1'^2 + \beta^2$ is purely real. It follows that

$$\beta'\beta'' + k_1'k_1'' = 0, \quad (1.24.1)$$

$$\tan \gamma_a = -\frac{\beta''}{k_1''} = \frac{k_1'}{\beta'} = -\cot \gamma_p. \quad (1.24.2)$$

Therefore, $\gamma_a = \frac{\pi}{2} + \gamma_p$, i.e., outside the layer, the phase and amplitude fronts of the surface wave are perpendicular to each other (Fig. 1-4). This is in agreement with the well-known property of inhomogeneous plane

waves propagating in lossless media. The angles γ_p and γ_a are shown in Figs. 1-5 and 1-6 as functions of frequency.

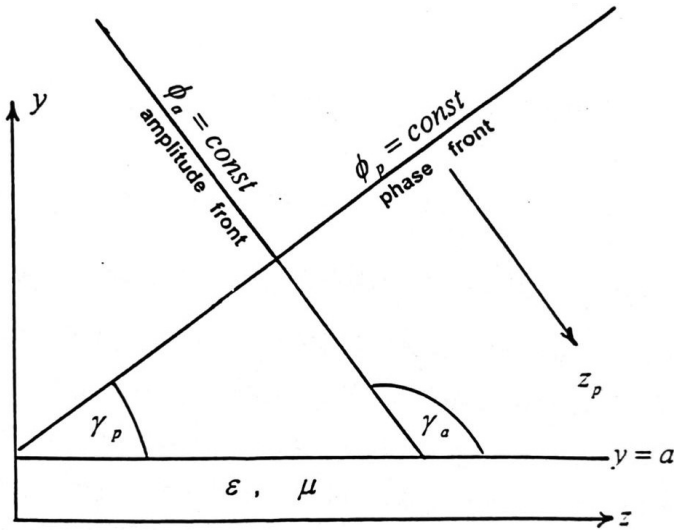


Fig. 1-4. Amplitude and phase fronts of the surface wave above the layer.

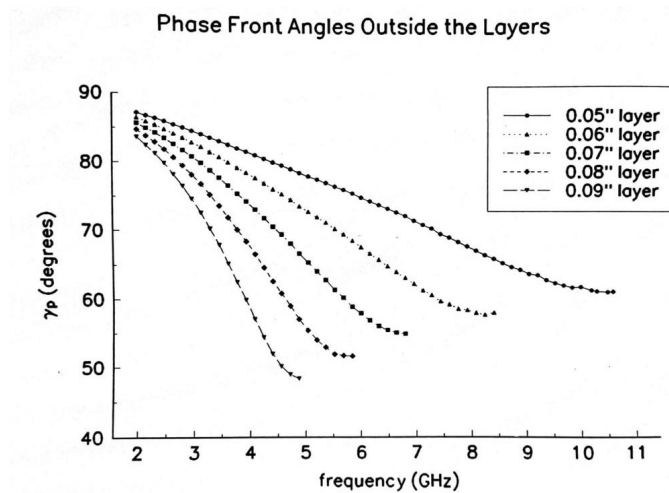


Fig. 1-5. Phase front angles of TM-waves outside the layers.

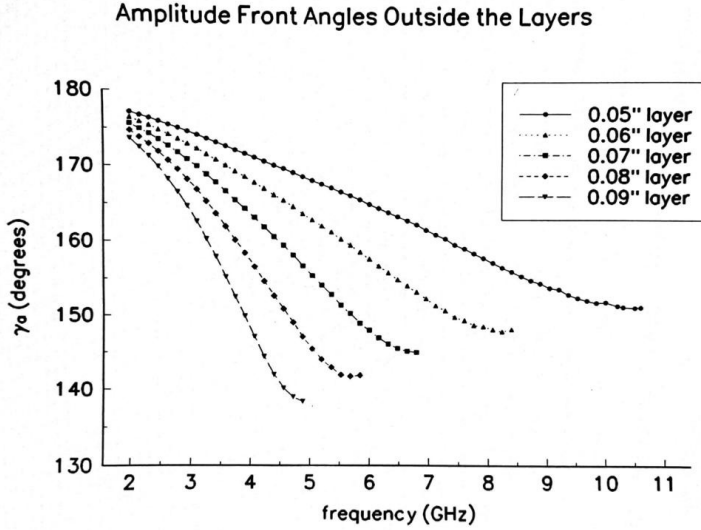


Fig. 1-6. Amplitude front angles of TM-waves outside the layers.

It is interesting to note a close connection between the angle γ_p and the complex Brewster angle $\gamma_B = \gamma'_B + i\gamma''_B$. The latter is introduced by the relation

$$e^{i(\beta z + k_1 y)} = e^{ik_0(z \sin \gamma_B - y \cos \gamma_B)} \quad (1.25)$$

where

$$\sin \gamma_B = \beta / k_0, \quad \cos \gamma_B = -k_1 / k_0. \quad (1.26)$$

From these equations it follows that $\sin \gamma'_B \cosh \gamma''_B = \beta' / k_0$, $\cos \gamma'_B \sinh \gamma''_B = \beta'' / k_0$, $\cos \gamma'_B \cosh \gamma''_B = -k'_1 / k_0$, $\sin \gamma'_B \sinh \gamma''_B = k''_1 / k_0$, and

$$\tan \gamma'_B = -\beta' / k'_1 = k''_1 / \beta'', \quad (1.27)$$